High-pressure phase transition of the oxonitridosilicate chloride Ce$_4$[Si$_4$O$_{3+x}$N$_{7-x}$]Cl$_{1-x}$O$_x$ with $x = 0.12$ and 0.18

Alexandra Friedrich[I], Karsten Knorr[*, II], Alexandra Lieb[III], Stephanie Rath[II], Michael Hanfland[IV], Bjoern Winkler[I] and Wolfgang Schnick[III]

[I] Institut für Mineralogie, Abt. Kristallographie, Johann Wolfgang Goethe-Universität Frankfurt, Senckenberganlage 30, D-60325 Frankfurt a. M., Germany
[II] Institut für Geowissenschaften, Mineralogie, Kristallographie, Christian-Albrechts-Universität zu Kiel, Olshausenstraße 40, D-24098 Kiel, Germany
[III] Department Chemie und Biochemie, Lehrstuhl für Anorganische Festkörperchemie, Ludwig-Maximilians-Universität München, Butenandtstraße 5–13 (D), D-81377 München, Germany
[IV] European Synchrotron Radiation Facility (ESRF), B.P. 220, F-38043 Grenoble Cedex, France

Dedicated to Professor Dr. Hans-Jörg Deiseroth on the occasion of his 60th birthday

Abstract.   The high-pressure behaviour of the oxonitridosilicate chlorides Ce$_4$[Si$_4$O$_{3+x}$N$_{7-x}$]Cl$_{1-x}$O$_x$, $x = 0.12$ and 0.18, is investigated by *in situ* powder synchrotron X-ray diffraction. Pressures up to 28 GPa are generated using the diamond-anvil cell technique. A reversible phase transition of first order occurs at pressures between 8 and 10 GPa. Within this pressure range the high- and the low-pressure phases are observed concomitantly. At the phase transition the unit cell volume is reduced by about 5%, and the cubic symmetry (space group $P2_13$) is reduced to orthorhombic (space group $P2_12_12_1$) following a *translationengleiche* group-subgroup relationship of index 3. A fit of a third-order Birch-Murnaghan equation of state to the $p-V$ data results in a bulk modulus $B_0 = 124(5)$ GPa with its pressure derivative $B' = 5(1)$ at $V_0 = 1134.3(4)$ Å^3 for the low-pressure phase and in $B_0 = 153(10)$ GPa with $B' = 3.0(6)$ at $V_0 = 1071(3)$ Å^3 for the high-pressure phase. The orthorhombic phase shows an anisotropic axial compression with the a axis (which is the shortest axis) being more compressible ($k(a) = 0.0143(4)$ 1/GPa) than the b and c axes ($k(b) = 0.0045(2)$, $k(c) = 0.0058(2)$ 1/GPa). The experimental results confirm an earlier prediction of the pressure-induced instability of isotypic Ce$_4$[Si$_4$O$_4$N$_6$]O, and also show that the bulk modulus was predicted reasonably well.

Introduction

Oxonitridosilicates are closely related to the common oxosilicates and nitridosilicates, the main difference being a partial replacement of oxygen by nitrogen, which is participating in the coordination of silicon (Schnick, Huppertz, Lauterbach, 1999; Schnick, 2001). Similarly to nitridosilicates, they are synthesised by high-temperature reactions, and show high chemical and thermal stability as well as mechanical hardness. However, only little is known about the high-pressure behaviour of nitridosilicates and related compounds, e.g., the binary compound Si$_3$N$_4$ has been investigated using *in situ* diamond-anvil cell techniques (Zerr, Miehe, Serghiou, Schwarz, Kroke, Riedel, Fueß, Kroll, Boehler, 1999). It was found that Si$_3$N$_4$ transforms to a new high-pressure polymorph at pressures above 15 GPa and temperatures exceeding 2000 K. The hardness of this phase has been suggested to be comparable to that of the hardest known oxides (Zerr et al., 1999). It is our aim to contribute to a better understanding of the material properties of nitridosilicates and related compounds by investigating their compressibility and stability at high pressure with respect to phase transitions, amorphisation or decomposition.

The structure of the oxonitridosilicate oxide Ce$_4$[Si$_4$O$_4$N$_6$]O is built up by SiON$_3$ tetrahedra, which are Q^3 type connected via corner-sharing nitrogen atoms forming a layer structure (Irran, Köllisch, Leoni, Nesper, Henry, Weller, Schnick, 2000). However, the layer is hyperbolically corrugated, which can explain the unexpected cubic symmetry (space group $P2_13$). [Ce$_4$O]$^{10+}$ cations fill the cavities with the Ce atoms being coordinated by the central oxygen atom of these tetrahedra as well as by the apex-oxygen atoms of the SiON$_3$ tetrahedra. Recently, a coupled substitution of chlorine for oxygen in the [Ce$_4$O]$^{10+}$ cations and of nitrogen for oxygen in the SiON$_3$ tetrahedra was achieved, hence partly forming [Ce$_4$Cl]$^{11+}$ cations and SiN$_4$ tetrahedra in the new Ce$_4$[Si$_4$O$_{3+x}$N$_{7-x}$]Cl$_{1-x}$O$_x$ compound (Lieb, Schnick, 2004).

* Correspondence author (e-mail: knorr@min.uni-kiel.de)

Quantum-mechanical density functional theory (DFT) based computations on $Ce_4[Si_4O_4N_6]O$ indicated structural instabilities and a possible phase transition at high pressures (Winkler, Hytha, Hantsch, Milman, 2001). Geometry optimisations at various pressures revealed a bulk modulus of $B_0 = 131(2)$ GPa from an equation-of-state fit to the computed $p-V$ data. However, when calculating the elastic constants by imposing finite strains, very large errors for a higher bulk modulus [$B_0 = 155(23)$ GPa] were obtained, which are thought to be due to the presence of local minima on the Born-Oppenheimer surface.

Here, $Ce_4[Si_4O_{3+x}N_{7-x}]Cl_{1-x}O_x$ is studied using powder X-ray diffraction at pressures up to 28 GPa, in order to determine its compressibility and to experimentally confirm the phase transition predicted for $Ce_4[Si_4O_4N_6]O$.

Experimental

Synthesis

Two samples of light-orange coloured oxonitridosilicate chloride $Ce_4[Si_4O_{3+x}N_{7-x}]Cl_{1-x}O_x$ were prepared following two different synthesis procedures, both being modifications of the method used by Irran et al. (2000). The compounds are representing substitutional variants of isotypic $Ce_4[Si_4O_4N_6]O$, resulting from a partial, coupled O/Cl- and O/N-implementation. Sample 1 was obtained by the reaction of cerium metal, silicon diimide ($Si(NH)_2$), a small amount of cerium chloride and silicon dioxide in a radiofrequency furnace at about 2050 K under nitrogen atmosphere. For the preparation of sample 2 cerium metal, cerium chloride, cerium oxides and silicon diimide were reacted at about 2070 K. The use of cesium chloride as a flux enhanced the formation of large single crystals. Single crystals were selected manually from a multiple-phase mixture using an optical microscope and then ground in an agate mortar.

Chemical analyses

Chemical analyses were performed on a Jeol Superprobe JXA-8900 electron-microprobe system (15 kV, 60 nA, 3 μm electron beam diameter, 40–180 s measurement time) at the Institute of Mineralogy, University of Frankfurt. $Ce_3Si_6N_{11}$ (Ce, N), wollastonite (Si), albite (O) and scapolite (Cl) were used as standard materials for calibration. A more detailed description of the quantitative wavelength-dispersive analyses will be given in a forthcoming publication (Lieb, Schnick, 2004).

Powder X-ray diffraction measurements

The two powder samples of $Ce_4[Si_4O_{3+x}N_{7-x}]Cl_{1-x}O_x$ with slightly different chlorine content were investigated at high pressures up to 28 GPa using a LeToullec diamond anvil cell with a gas driven membrane for pressure generation. Neon was loaded as the pressure-transmitting medium in an autoclave. Holes serving as sample chambers (150 μm in diameter) were drilled through inconel gaskets (pre-indented to a thickness of 40 μm) using a spark-erod-

ing drilling machine. Pressure was determined by means of the laser-induced ruby-fluorescence technique (Mao, Bell, Shaner, Steinberg, 1978) before and after each exposure. *In situ* high-pressure synchrotron X-ray powder diffraction data were collected at the ID9A high-pressure station of the ESRF at a wavelength of 0.4138 Å using a MAR345 online image plate scanner. A sample-to-detector distance of 362 mm allowed data collection up to about $2\theta = 24°$ giving a maximum $\sin\theta/\lambda$ of 0.502 Å^{-1}.

Full powder-diffraction images were processed and integrated using FIT2D (Hammersley, Svensson, Hanfland, Fitch, Häusermann, 1996). Single diffraction spots from the sample and the pressure medium were masked and thus excluded from integration. Cell parameters were refined with the General Structure Analysis System (GSAS; Larson, Von Dreele, 1994).

Results and discussion

An average over 19 point analyses with the electron microprobe (Table 1), normalised to Si = 4, yielded a chlorine content of 3.4(2) wt% for sample 1 and 3.7(1) wt% for sample 2. This gives x-values of 0.18(3) and 0.12(2) for sample 1 and sample 2, respectively.

Unit cell parameters as a function of pressure are summarised in Tables 2 and 3. The orthorhombic unit cell of the high-pressure phase (space group $P2_12_12_1$, no. 19) was determined using the program TREOR90 (Werner, Eriksson, Westdahl, 1985; modified 1990). The metric of this orthorhombic cell corresponds to that of the cubic phase (*translationengleiche* subgroup). The reflection conditions for the three 2_1 axis are fulfilled. Unit cell volume and cell axes are plotted as a function of pressure in Figs. 1 and 2.

The small difference in the unit cell parameter of the two samples of $Ce_4[Si_4O_{3+x}N_{7-x}]Cl_{1-x}O_x$ at ambient pressure was confirmed from the refinement of powder diffraction patterns of two independent cell loadings. The unit cell parameter of sample 1 ($a = 10.426(1)$ Å) is smaller by $\approx 0.07\%$ than that of sample 2 ($a = 10.433(2)$ Å). The incorporation of chlorine is expected to lead to an increase of the unit cell parameter compared to $a = 10.3546(6)$ Å of $Ce_4[Si_4O_4N_6]O$ (Irran et al., 2000). Assuming an occupancy of the chlorine atom position of 88(2)% for sample 2 as resulting from electron-microprobe analyses (Table 1), the chlorine content of sample 1 is estimated to be 80(2)% based on a linear extrapolation of the unit cell

Table 1. Results of electron-microprobe analyses of samples 1 and 2 of $Ce_4[Si_4O_{3+x}N_{7-x}]O_xCl_{1-x}$.

p/GPa	sample 1		sample 2	
	wt%	normalised	wt%	normalised
Si	13.3(1)	4	13.3(1)	4
Ce	64.8(4)	3.90(5)	66.2(2)	4.00(5)
Cl	3.4(1)	0.82(3)	3.7(1)	0.88(2)
N	11.5(2)	6.95(6)	11.6(2)	7.00(6)
O	6.1(2)	3.23(6)	6.0(1)	3.15(5)
Sum	99.2(4)	18.9	100.6(3)	19.0

Table 2. Pressure dependence of the unit cell parameters of sample 1 of $Ce_4[Si_4O_{3+x}N_{7-x}]O_xCl_{1-x}$, $x = 0.18$. Only the a cell parameter is given for the cubic low-pressure phase, the a, b and c cell parameters for the orthorhombic high-pressure phase. Values from decompression measurements are marked by asterisks.

p/GPa	a/Å	b/Å	c/Å	V/Å^3
0.0001	10.4255(1)			1133.17(4)
0.383(2)	10.4138(1)			1129.36(4)
3.226(5)	10.33768(6)			1104.76(2)
4.402(7)	10.31185(7)			1096.50(2)
6.307(8)	10.26494(6)			1081.61(2)
6.56(4)	10.2659(3)			1081.92(8)*
8.25(2)	10.2247(1)			1068.93(4)
8.30(1)	10.2272(3)			1069.71(9)
8.501(2)	10.2243(3)			1068.81(8)
8.758(4)	10.2194(2)			1067.26(7)
8.88(5)	8.9995(4)	10.4815(4)	10.7777(5)	1016.64(5)*
8.97(1)	10.21437(9)			1065.70(3)
	8.975(1)	10.483(1)	10.764(1)	1012.7(1)
9.034(8)	10.2127(1)			1065.17(3)
	8.973(1)	10.473(1)	10.773(1)	1012.4(1)
9.534(8)	10.2030(4)			1062.2(1)
	8.9689(6)	10.4683(6)	10.7863(6)	1012.72(7)
10.24(2)	8.9573(5)	10.4580(6)	10.7469(5)	1006.73(7)
10.444(1)	8.9424(4)	10.4585(5)	10.7523(6)	1005.60(6)
10.758(8)	8.9349(2)	10.4577(3)	10.7431(3)	1003.82(3)
12.49(1)	8.8938(4)	10.4354(5)	10.7183(5)	994.77(6)
14.11(1)	8.8429(4)	10.4154(4)	10.7025(5)	985.72(5)
14.76(2)	8.8401(4)	10.4062(6)	10.6896(8)	983.36(7)*
16.206(2)	8.8042(4)	10.3933(4)	10.6677(4)	976.14(5)
17.680(4)	8.7647(6)	10.3691(5)	10.6514(5)	968.02(6)
19.90(3)	8.7024(5)	10.3598(5)	10.6088(5)	956.44(5)
22.10(2)	8.649(1)	10.3532(9)	10.553(1)	945.0(1)
26.160(6)	8.6050(8)	10.2819(6)	10.5250(9)	931.20(9)*
26.75(1)	8.5926(7)	10.2658(5)	10.5156(7)	927.57(8)
28.21(1)	8.5811(8)	10.2389(8)	10.5053(8)	923.0(1)

Table 3. Pressure dependence of the unit cell parameters of sample 2 of $Ce_4[Si_4O_{3+x}N_{7-x}]O_xCl_{1-x}$, $x = 0.12$. Only the a cell parameter is given for the cubic low-pressure phase, the a, b and c cell parameters for the orthorhombic high-pressure phase. Values from decompression measurements are marked by asterisks.

| p/GPa	a/Å	b/Å	c/Å	V/Å^3
0.0001	10.43169(8)			1135.18(3)
0.340(2)	10.41904(8)			1131.06(3)
2.368(2)	10.36989(9)			1115.12(3)*
3.429(7)	10.34254(7)			1106.32(2)
4.877(3)	10.30782(8)			1095.22(3)
6.10(2)	10.27724(8)			1085.50(3)
6.5(1)	10.2726(2)			1084.02(7)*
8.490(4)	10.22506(7)			1069.05(2)
9.06(1)	10.21402(9)			1065.59(3)
9.86(1)	10.2012(5)			1061.6(2)
	8.9558(4)	10.4701(6)	10.7840(6)	1011.20(6)
11.32(1)	8.9106(4)	10.4542(6)	10.7654(6)	1002.83(6)
14.38(2)	8.8298(3)	10.4111(3)	10.7192(4)	985.39(3)
16.079(5)	8.7912(4)	10.3974(4)	10.6929(4)	977.39(4)*
18.290(2)	8.7497(4)	10.3576(4)	10.6620(4)	966.25(4)
20.900(8)	8.6959(5)	10.3423(6)	10.6188(6)	955.01(5)
23.95(1)	8.6512(5)	10.2987(6)	10.5740(6)	942.10(6)
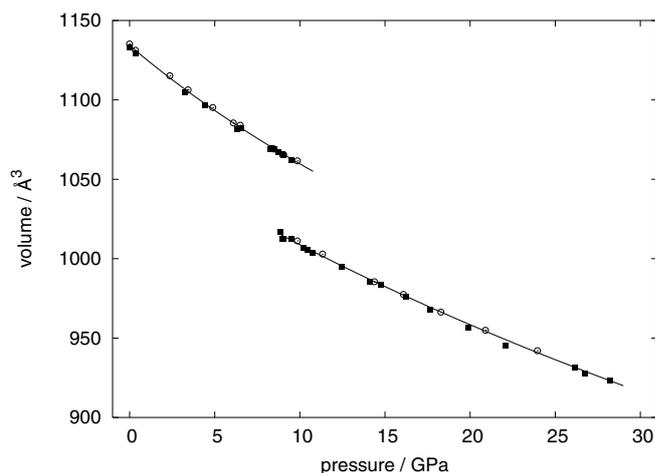
Fig. 1. Pressure dependence of the unit cell volumes of samples 1 (solid squares; $x = 0.18$) and 2 (open circles; $x = 0.12$) of $Ce_4[Si_4O_{3+x}N_{7-x}]Cl_{1-x}O_x$. Standard deviations are smaller than symbols. A discontinuity in the pressure dependence of the unit cell volume at pressures around 9 GPa indicates the occurrence of a first-order phase transition. Equation-of-state fits to data of the low- and the high-pressure phases are represented by solid lines.

parameters as a function of chlorine content between the chlorine-free end-member (Irran et al., 2000) and sample 2. This estimation is in good agreement with the experimentally determined chlorine content of 82(3)% for sample 1 (Table 1).

Phase transition

The experiments are in accordance with the proposed instability of this compound at high pressure (Winkler et al., 2001). A reversible phase transition occurring in the pressure range between 8 and 10 GPa was detected. The phase transition was accompanied by a distinct change of the powder diffraction pattern and by a reduction of the cubic symmetry (Fig. 3). We observed a discontinuity in the pressure dependence of the unit cell volume (Fig. 1) as well as in all of the unit cell axes (Fig. 2), which is char-
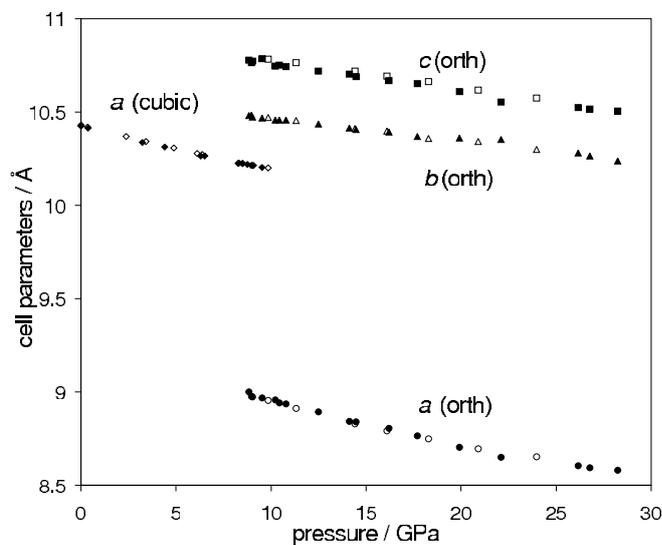
Fig. 2. Unit cell axes of the cubic low-pressure and the orthorhombic (orth) high-pressure phase as a function of pressure. Sample 1 is represented by filled symbols, sample 2 by open symbols.
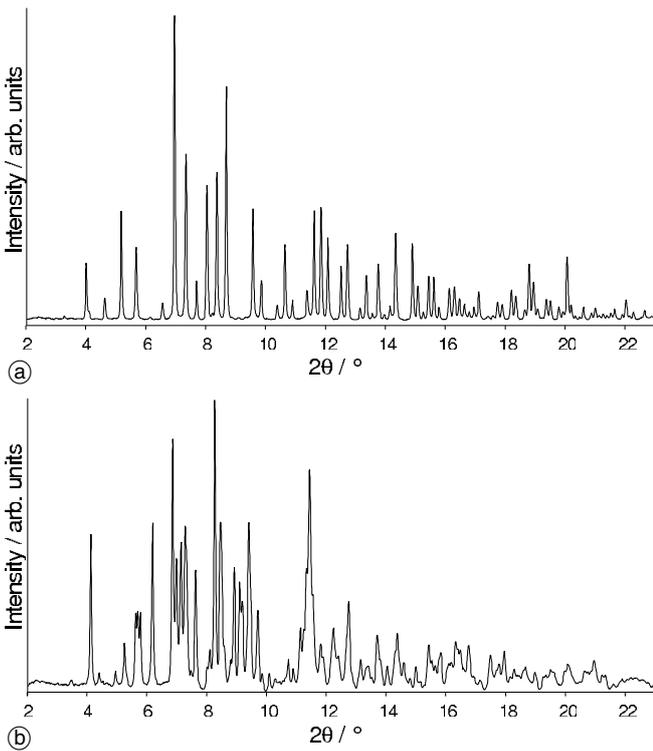
Fig. 3. Powder diffraction pattern of (**a**) cubic (9.06 GPa) and (**b**) orthorhombic (11.32 GPa) $Ce_4[Si_4O_{3+x}N_{7-x}]Cl_{1-x}O_x$ (sample 2) after subtraction of the background, mainly originating by Compton scattering of the diamond anvils, using a Chebyshev function.

acteristic for a first-order phase transition. The decrease of the cell volume $[(V_{cubic} - V_{orth})/V_{cubic}]$ amounts to $\approx 5\%$ at the phase transition. Following a *translationengleiche* group-subgroup relationship of index 3 the space group symmetry $P2_13$ is reduced to $P2_12_12_1$ ($a_{orth} = 8.9573(5)$, $b_{orth} = 10.4580(6)$, $c_{orth} = 10.7469(5)$ Å, at 10.24(2) GPa; sample 1). Within a pressure range of about two GPa both the cubic and the orthorhombic phases were observed concomitantly. In sample 1 the high-pressure phase started to appear at ≈ 8.3 GPa, became dominant at 9.5 GPa and was the only component from 10.2 GPa to the highest pressure obtained. In sample 2, however, the phase transformation started at slightly higher pressures around 9.1 GPa, showing a phase mixture at 9.9 GPa and a pure high-pressure phase at 11.3 GPa. As sample 2 contains slightly more chlorine, the chlorine content seems to increase the transition pressure. At pressure release a hysteresis down to 8.8 GPa was observed in sample 1, which again confirms the first-order character of the phase transition.

Compressibility

Pressure-volume data of the low- and the high-pressure phase, respectively, were fitted by a third-order Birch-Murnaghan equation of state (BM-EOS) using the program EOS-FIT (Angel, 1998) and a fully weighted least-squares procedure (Fig. 1). Fits of separate equations of state to each of the two samples could not be used to investigate the influence of the coupled O/Cl- and O/N-substitution on the compressibility due to an insufficient accuracy. The limited number of pressure points available for each sam-

ple does not cover the pressure range evenly and, thus, results in strongly deviating values for the pressure derivative of the bulk modulus, B', and further the bulk modulus, B_0, itself, which would suggest much larger substitution effects than recognisable from the data graphs. Hence, we decided to fit one equation to the data of both samples 1 and 2. This leads to reliable averaged results. The numerical uncertainty of the results is only slightly increased by this procedure as the cell dimensions of the two samples differ significantly, but as the difference is less than 1%, this can be neglected.

The values obtained for the cubic low-pressure phase are $B_0 = 124(5)$ GPa and $B' = 5(1)$ with $V_0 = 1134.3(4)$ Å^3. The bulk modulus is similar to the theoretically predicted bulk moduli of isotypic oxonitridosilicate oxide $Ce_4[Si_4O_4N_6]O$ with $B_0 = 131(2)$ GPa and $B' = 5.0(2)$ at $V_0 = 1113.9$ Å^3 and the oxonitridoalumosilicate $SrSiAl_2O_3N_2$ with $B_0 = 131.9(3)$ GPa (Winkler et al., 2001). The slightly larger bulk modulus of chlorine-free $Ce_4[Si_4O_4N_6]O$ is still comparable to that of the chlorine-bearing $Ce_4[Si_4O_{3+x}N_{7-x}]Cl_{1-x}O_x$ within two standard deviations. However, this difference seems reasonable due to the smaller unit-cell volume at ambient pressure. Further, larger cations are more compressible and, hence, the observed behaviour is consistent with the substitution of chlorine by oxygen (Hazen, Finger, 1982).

Fitting a 3rd-order BM-EOS to the $p-V$ data of the high-pressure phase results in $B_0 = 153(10)$ GPa and $B' = 3.0(6)$ at $V_0 = 1071(3)$ Å^3. The extrapolated unit cell volume at ambient pressure is smaller by about 5.6% compared to that of the low-pressure phase. This is quite reasonable considering a difference in volume of about 5% at the phase transition. The high-pressure phase is less compressible than the low-pressure phase and shows a smaller pressure derivative of the bulk modulus. This corresponds to the usually expected behaviour as the repulsive forces of atoms become stronger at decreasing distances. Further, the sudden strong reduction of the unit-cell volume is responsible for an increase of the bulk modulus at the phase transition pressure. From the corresponding equations of state the bulk modulus at 9 GPa is calculated to be $B = 169$ GPa for the low-pressure phase and $B = 180$ GPa for the high-pressure phase.

Normalised $a(p)$, $b(p)$ and $c(p)$ data of the high-pressure phase were fitted with a 2nd-order BM-EOS using a unit weighted least-squares procedure. From the fits we obtain the linear compressibilities $k = 1/(3B_0)$: $k(a) = 0.0143(4)$ 1/GPa, $k(b) = 0.0045(2)$ 1/GPa and $k(c) = 0.0058(2)$ 1/GPa. The anisotropy of the orthorhombic phase shows a surprising behaviour, as the most deformed and shortest a axis continues to be the by far most compressible one on further pressure increase, while the b and c axes are compressed at a lower rate with the c axis being more compressible than the b axis.

Conclusions

The experiments described here have addressed a number of open questions concerning the physical properties of nitridosilicates, e.g., the compressibility and the phase sta-

bility at high pressure. We have confirmed the presence of a pressure-induced phase transformation, which had previously been speculated about. We have also confirmed that predictions about the compressibility were reasonably accurate. Further open questions remain, of which the most obvious one is the anomalous behaviour of the compressibilities of the individual lattice parameters. Here, high-pressure single-crystal diffraction experiments are required to understand the detailed compression mechanism, and such experiments are currently being performed. Furthermore, the phase transition is accompanied by a discontinuous colour change from orange to dark red, and in preliminary micro-Raman spectroscopic data some, as yet unexplained, changes have also been observed. The present study will therefore serve as a basis for further investigations of the pressure-dependence of the structure – property relationships of this very interesting class of compounds.

References

Angel, R.: Program EOS-FIT, version 4.2 (1998).

Hammersley, A. P.; Svensson, S. O.; Hanfland, M.; Fitch, A. N.; Häusermann, D.: Two-dimensional detector software: From real detector to idealised image or two-theta scan. High Pressure Res. **14** (1996) 235–248.

Hazen, R. M.; Finger, L. W.: Comparative Crystal Chemistry. John Wiley & Sons, Chichester, New York, Brisbane, Toronto, Singapore 1982.

Irran, E.; Köllisch, K.; Leoni, S.; Nesper, R.; Henry, P. F.; Weller, M. T.; Schnick, W.: $Ce_4[Si_4O_4N_6]O$ – A hyperbolically layered oxonitridosilicate oxide with an ordered distribution of oxygen and nitrogen. Chem. Eur. J. **6** (2000) 2714–2720.

Larson, A. C.; Von Dreele, R. B.: Los Alamos National Laboratory Report LAUR (1994) 86–748.

Lieb, A.; Schnick, W.: (2004) unpublished.

Mao, H.; Bell, P.; Shaner, J.; Steinberg, D.: Specific volume measurement of Cu, Mo, Pd, and Ag and calibration of the ruby R_1 fluorescence pressure gauge from 0.06 to 1 Mbar. J. Appl. Phys. **49** (1978) 3276–3283.

Schnick, W.: Nitridosilicates, oxonitridosilicates (sions), and oxonitridoaluminosilicates (sialons). New Materials with promising properties. Int. J. Inorg. Mater. **238** (2001) 28–35.

Schnick, W.; Huppertz, H.; Lauterbach, R.: High temperature syntheses of novel nitrido- and oxonitrido-silicates and sialons using rf furnaces. J. Mater. Chem. **9** (1999) 289–296.

Werner, P.-E.; Eriksson, L.; Westdahl, M.: TREOR, a semi-exhaustive trial-and-error powder indexing program for all symmetries. J. Appl. Crystallogr. **18** (1985) 367–370.

Winkler, B.; Hytha, M.; Hantsch, U.; Milman, V.: Theoretical study of the structures and properties of $SrSiAl_2O_3N_2$ and $Ce_4[Si_4O_4N_6]O$. Chem. Phys. Lett. **343** (2001) 622–626.

Zerr, A.; Miehe, G.; Serghiou, G.; Schwarz, M.; Kroke, E.; Riedel, R.; Fueß, H.; Kroll, P.; Boehler, R.: Synthesis of cubic silicon nitride. Nature **400** (1999) 340–342.